Complexation of Na^+ in Redox-Active Ferrocene Crown Ethers, a Structural Investigation, and an Unexpected Case of Li^+ Selectivity

Herbert Plenio*,† and Ralph Diodone

Institut für Anorganische und Analytische Chemie, Universität Freiburg, Albertstr. 21, 79104 Freiburg, Germany

Received December 21, 1994[⊗]

The synthesis of several ferrocene crown ethers is described, which were designed to selectively coordinate and recognize electrochemically small group 1 ions sandwiched between two 12-membered crown ether rings. The reactions of the [1,1′-ferrocenediylbis(methylene)]bis[pyridinium] salt [Fcdiyl(py)$_2^{2+}$] with diaza-12-crown-4 [H(N$_2$-12-C-4)H], aza-12-crown-4 [H(N-12-C-4)], and 1,2-ethanediylbis(1,7-dioxa-4,10-diazacyclododecane) [C$_2$H$_4$diyl-((N$_2$-12-C-4)H)$_2$] yielded the respective ferrocene crown ethers 1,1″:1′,1‴-bis(ferrocenediyl)bis[4,10-bis(methylene)-1,7-dioxa-4,10-diazacyclododecane)] [Fcdiyl(N$_2$-12-C-4)$_2$Fcdiyl] (**3**), [Fcdiyl(N-12-C-4)$_2$] (**2**), and [Fcdiyl(N$_2$-12-C-4)$_2$(C$_2$H$_4$diyl)] (**4**). Complexation of group 1 ions was evidenced by NMR, cyclic voltammetry, FAB mass spectrometry, and picrate extraction experiments. This last techniques was used to determine a complexation selectivity of **4** for $Li^+/Na^+ \approx 20:1$. The redox potentials of the ligands **2**, **3**, and **4** were determined by cyclic voltammetry; addition of Li^+ or Na^+ results in anodic shifts of the redox potentials of up to 100 mV for (**4**)Na^+ and 140 mV for (**4**)Li^+. The X-ray crystal structures of [(**2**)NaClO$_4$]$_2$, [(**2**)NaBPh$_4$]$_2$, **3**, **3**·2HClO$_4$, **4**, and (**4**)NaI were determined to understand the coordination behavior of these ligands and the metal ion selectivities displayed. The determining factor for the stability of the metal complexes is the orientation of the plane of the cyclopentadienyl (Cp) ring with respect to the Cp**C**H$_2$−**N** vector. In metal ion or proton complexes torsion angles of close to 90° are preferred, which allow the equal participation of all donor atoms in the coordination of a cation. This property, however, prevents the complexation of Na^+ or Li^+ within the cavity formed by **3**. Replacing one 1,1′-ferrocenediylbis(methylene) group in **3** by a sterically more suitable C$_2$H$_4$ bridge results in **4** and allows formation of the Na^+-sandwich (**4**)NaI. In this complex strain is apparent, which leads to the preferential coordination of Li^+ by **4**. The results obtained in this study make it possible to set up a correlation of the anodic shifts ΔE of the iron redox potentials upon complexation of Na^+ by ferrocene crown ethers and the inverse distance Fe−Na^+ as determined by crystal structure analysis $\Delta E \cong 1/(Fe-Na^+)$. This indicates that crystal structures of metal complexes of ferrocene crown ethers can serve as reasonable models for the corresponding species in solution.

Introduction

The remarkable ability of macrocycles to selectively coordinate metal ions complementary in size to the diameter of the cavity formed by the donor atoms is of fundamental importance to coordination chemistry.[1] However, the ability of monocyclic crown ethers (coronands) to distinguish between different metal ions is often overestimated since these rings still possess a high degree of conformational flexibility.[2] Cram's work on rigid ligands such as spherands has established that preorganization, i.e. the orientation of the donor atoms in the free ligand as required for the coordination of metal ions, is very important to achieve high stability constants and ion selectivities.[3] However, it should be borne in mind that the optimization of thermodynamic stability finally leads to macrocycle−metal complexes which display extremely small rates for complexation and/or decomplexation reactions.[4] Such kinetically hindered systems are not very useful with respect to the application of macrocycles in areas such as membrane transport[5] or chemical sensors.[6] Nature herself has long recognized this problem, and for this very reason the ionophore Valinomycin, a depsipeptide, represents an excellent compromise between a highly flexible depside (good selectivity, fast kinetics) and a rigid peptide such as Prolinomycin (excellent selectivity, slow kinetics).[7] In this intermediate region factors other than simple size-match relationships or the attainment of the preferred M−O bond lengths determine the relative stability of metal complexes.[8] It is increasingly being recognized by evidence obtained from molecular modeling studies and experimental work that factors like the solvation of the anion, the chelate ring size, a trigonal-planar geometry around oxygen, and the basicity and nature of donor atoms are crucial in determining complex stabilities and hence selectivities.[9] We were interested therefore in the synthesis of crown ethers which are able to selectively coordinate small metal ions and also contain a redox-active center able to electrochemically detect the presence of this metal ion.[10] The starting points of this project are that Na^+—in contrast to

† E-mail plenio@sun8.ruf.uni-freiburg.de.

⊗ Abstract published in *Advance ACS Abstracts*, June 15, 1995.

(1) (a) Dietrich, B.; Viout, P.; Lehn, J. M. *Macrocyclic Chemistry*; VCH: Weinheim, Germany, 1993. (b) Gokel, G. W. *Crown Ethers and Cryptands*; Royal Soc. of Chem: London, 1991.
(2) Hancock, R. D. In *Crown Ether Compounds*; Cooper, S. R., Ed.; VCH: Weinheim, Germany, 1992; Chapter 10.
(3) Cram, D. J. *Angew. Chem.* **1986**, *98*, 1041; *Angew. Chem., Int. Ed. Engl.* **1986**, *25*, 1039.
(4) Cram, D. J.; Lein, G. M. *J. Am. Chem. Soc.* **1985**, *107*, 3657.
(5) vanStraten-Nijenhuis, W. F.; deJong, F.; Reinhoudt, D. N. *Receuil* **1993**, *112*, 317.
(6) (a) Cobben, P. L. H. M.; Egeberink, R. J. M.; Bomer, J. G.; Bergveld, P.; Verboom, W.; Reinhoudt, D. N. *J. Am. Chem. Soc.* **1992**, *114*, 10573. (b) Misumi, S. *Top. Curr. Chem.* **1993**, *165*, 165. (c) Takagai, M.; Nakano, K.; Nakashima, N. *Pure Appl. Chem.* **1989**, *61*, 1605. (d) Marsella, M. J.; Swager, T. M. *J. Am. Chem. Soc.* **1993**, *115*, 12214. (e) deSilva, A. P.; Gunaratne, H. Q. N.; McCoy, C. P. *Nature* **1993**, *364*, 42.
(7) (a) Gokel, G. W. In *Crown Compounds*, Cooper, S. R., Ed.; VCH: Weinheim, Germany, 1992; Chapter 1. (b) Marrone, T. J.; Merz, K. M. *J. Am. Chem. Soc.* **1995**, *117*, 779.
(8) Christensen, J. J.; Bradshaw, J. S.; Nielsen, S. A.; Izatt, R. M. *Chem. Rev.* **1974**, *74*, 351.

0020-1669/95/1334-3964$09.00/0

K^+—forms stable complexes with 12-membered crown ethers such that Na^+ is sandwiched between two crown ether rings[11] and that we have recently described a facile synthesis of ferrocene crown ethers.[12] Our target therefore was to synthesize ferrocene crown ethers containing two 12-membered crown ether units. The small cavity formed should be predisposed to coordinate small group 1A ions in close proximity to the redox-active ferrocene moiety. Such compounds might also be useful for the redox-switched bonding of Li^+ or Na^+ since the oxidation of the ferrocene unit creates a positive charge close to the crown ether bound cation leading to a destabilization of the crown ether complex.[13,14]

Experimental Section

Commercially available solvents and reagents were purified according to literature procedures. Chromatography was carried out with silica MN 60. NMR spectra were recorded at 300 K with a Bruker AC200 F (^{1}H NMR 200 MHz, ^{13}C NMR 50 MHz) or a Varian Unity 300 (^{1}H NMR 300 MHz, ^{13}C NMR 75 MHz). ^{1}H NMR was referenced to residual hydrogen impurities in the solvent, and ^{13}C NMR, to the solvent signals: $CDCl_3$ (7.26 ppm, 77.0 ppm) and CD_3CN (1.93 ppm, 1.30 ppm). Elemental analyses were performed by the Mikroanalytisches Labor der Chemischen Laboratorien, Universitat. Freiburg. Melting points were determined with a Meltemp melting point apparatus in sealed capillaries. Starting materials were commercially available or prepared according to literature procedures: [1,1′-ferrocenediylbis(methylene)]bis[pyridinium] chloride tosylate,[15] 1,1′-ferrocenediylbis-[7,16-bis(methylene)-10-aza-1,4,7-trioxacyclododecane].[12] For the synthesis of 1,2-ethanediylbis(1,7-dioxa-4,10-diazacyclododecane) we initially had followed a procedure by Calverly and Dale.[16] However, we encountered problems with the debenzylation reaction with H_2—Pd/C in the last step of the synthesis of this bis(crown), since the yields often were very poor. We found it much easier to cleave the benzyl group by room-temperature reaction in HCOOH—Pd/C for 14 d.[17] This procedure gave quantitative yields of the debenzylated product. Picrate salts were prepared according to literature procedures.[18]

Picrate extraction experiments were carried out according to a procedure by Cram et al. and were validated by performing the experiments under the same conditions, used to reproduce the literature values for dicyclohexano-18-C-6.[19] FAB-MS/mass spectra were recorded on a Finnigan MAT 8230. Mixtures of 1 equiv of the respective ferrocene crown ether and 1 equiv of each of the perchlorates of Li^+, Na^+, K^+, and Rb^+ were mixed in 3-nitrobenzyl alcohol and equilibrated for 60 min, and 1 μL of the solution was applied to the FAB probe. NMR determinations of metal ion selectivities were carried out by recording the ^{1}H and ^{13}C NMR spectra of an equimolar mixture of the respective metal perchlorates and ferrocene crown ether. The ratio of the integrals or peak heights of the respective metal complexes determine the selectivity. Cyclic voltammetry: The standard electrochemical instrumentation consisted of a Amel System 5000 potentiostat/galvanostat. Cyclic voltammograms were recorded in dry CH_3CN under an argon atmosphere at −30 °C or ambient temperature using Amel software on a PC. A three-electrode configuration was employed. The working electrode was a Pt disk (diameter 1 mm) sealed in soft glass. The counter electrode was a Pt disk (area 3 cm^2). The pseudoreference electrode was an Ag wire. Potentials were calibrated against the formal potential of cobaltocenium perchlorate (−0.94 V vs Ag/AgCl). NBu_4PF_6 (0.1 M) was used as a supporting electrolyte.

Fcdiyl(N_2-12-C-4)$_2$Fcdiyl (3). 4,10-Diaza-1,7-dioxacyclododecane (0.40 g, 2.28 mmol), [1,1′-ferrocenediylbis(methylene)]bis[pyridinium] chloride tosylate (1.32 g, 2.28 mmol), and 0.3 g of Na_2CO_3 were dissolved in 150 mL of CH_3CN and heated under reflux for 24 h. The cold solution was filtered and washed with CH_3CN, and the solvent was evaporated. The oily residue was dissolved in 40 mL of CH_2Cl_2 and washed twice with 20 mL of water. The organic layer was separated, dried over $MgSO_4$, and filtered, and the solvent was removed in vacuo. Chromatographic purification followed (silica, cyclohexane/diethylamine = 10:1). Yield: 0.087 g (10%). Mp: 177 °C. ^{1}H NMR ($CDCl_3$): δ 2.74 (t, J = 4.8 Hz, 16H, NCH_2), 3.62 (t, J = 4.9 Hz, 16H, OCH_2), 3.65 (s, CH_2Cp), 4.08 ("t", J = 1.8 Hz, 8H, Fc), 4.18 ("t", J = 1.8 Hz, 8H, Fc). ^{1}H NMR ($CDCl_3$/CD_3CN, 2:1): δ 2.68 (t, J = 4.7 Hz, 16H, NCH_2), 3.57 (t, J = 4.7 Hz, 16H, OCH_2), 3.60 (s, CH_2Cp), 4.04 ("t", J = 1.7 Hz, 8H, Fc), 4.15 ("t", J = 1.7 Hz, 8H, Fc). ^{13}C NMR ($CDCl_3$): δ 53.88, 54.53, 68.25, 69.35, 70.30, 84.97. ^{13}C NMR ($CDCl_3$/CD_3CN, 2:1): δ 54.08, 54.51, 68.39, 69.43, 70.41, 85.44. FAB-MS [*m/e* (% relative intensity)]: 769 (M + H^+, 85%), 664 (100%). Anal. Calcd for $C_{40}H_{56}Fe_2N_4O_4$ (768.6): C, 62.51; H, 7.34. Found: C, 62.66; H, 7.33.

(3)NaBPh$_4$. ^{1}H NMR ($CDCl_3$/CD_3CN, 2:1): δ 2.61 (t, J = 4.3 Hz, 16H, NCH_2), 3.50 (t, J = 4.6 Hz, 16H, OCH_2), 3.59 (s, CH_2Cp), 4.08 ("t", J = 1.7 Hz, 8H, Fc), 4.18 ("t", J = 1.7 Hz, 8H, Fc). ^{13}C NMR ($CDCl_3$/CD_3CN, 2:1): δ 52.85, 55.59, 68.08, 69.32, 69.96, 83.04.

Fcdiyl(N_2-12-C-4)$_2$(C_2H_4diyl) (4). A mixture of 1,2-ethanediylbis-(1,7-dioxa-4,10-diazacyclododecane) (0.30 g, 0.8 mmol), Li_2CO_3 (0.5 g), and [1,1′-ferrocenediylbis(methylene)]bis[pyridinium] chloride tosylate (0.46 g, 0.8 mmol) in CH_3CN (100 mL) was heated under reflux for 16 h. The cold reaction mixture was filtered and the solvent evaporated. The residue was taken up in 25 mL of CH_2Cl_2, and washed twice with 10 mL of aqueous KOH. The organic layer was separated, dried over $MgSO_4$, filtered, and evaporated. The residue was chromatographed on silica (cyclohexane/diethylamine) = 10:1). **4** was obtained as a yellow solid: mp 91 °C; yield 110 mg (24%). ^{1}H NMR ($CDCl_3$): δ 2.65−2.70 (m, 12 H, NCH_2), 2.78 (t, J = 5.0 Hz, 8H, NCH_2), 3.55 (s, 4H, $FcCH_2$), 3.6−3.7 (m, 16H, OCH_2), 3.98 ("t", J = 1.8 Hz, 4H, FcH), 4.16 ("t", J = 1.8 Hz, 4H, FcH). ^{13}C NMR ($CDCl_3$): δ 54.99, 55.07, 55.34, 68.27, 69.17, 69.34, 69.90, 86.34. Anal. Calcd for $C_{30}H_{48}FeN_4O_4$ (584.58): C, 61.64; H, 8.28; N, 9.58. Found: C, 61.56; H, 8.22; N, 9.87.

(4)LiClO$_4$. ^{1}H NMR (CD_3CN): δ 2.45−2.73 (m, NCH_2), 2.62 (s, NCH_2), 2.85 (t, J = 5.5 Hz, NCH_2), 3.55−3.85 (m, OCH_2 + NCH_2, 16H + 4H), 4.08 ("t", J = 1.7 Hz, FcH), 4.13 ("t", J = 1.7 Hz). ^{13}C NMR (CD_3CN) gave extremely broad lines between 270 and 330 K.

(4)NaClO$_4$. ^{1}H NMR (CD_3CN): δ 2.56 (s, NCH_2), 2.59−2.73 (m, NCH_2), 3.47−3.65 (m, OCH_2), 3.76−3.86 (m, OCH_2), 3.81 (s, $FcCH_2$), 4.10 (s, FcH). ^{13}C-NMR (CD_3CN): δ 53.11, 53.36, 54.21, 56.44, 68.30, 69.13, 70.28, 71.10, 85.24.

(4)KClO$_4$. ^{1}H NMR (CD_3CN): δ 2.58 (br s, NCH_2), 2.7 (vbr, NCH_2), 3.46 (s), 3.5−3.7 (vbr), 4.14 (FcH). ^{13}C NMR (CD_3CN): δ 51.87, 53.35, 54.09, 58.97, 67.68, 68.30, 69.57, 72.08, 85.63.

X-ray Crystal Structure Determinations. X-ray data were collected on an Enraf-Nonius CAD4 diffractometer using a graphite monochromator and Mo Kα or Cu Kα radiation. An empirical absorption correction (ψ-scans) was applied in all cases. Structure solution and refinement was carried out using SHELXS-86 and SHELXL-93[20] (Table 1). The data for all the structures (except [(**2**)-$NaBPh_4]_2$) were deposited and are available at the Fachinformationszentrum Karlsruhe, D-76344 Eggenstein-Leopoldshafen, Germany,

(9) (a) Hancock, R. D.; Martell, A. E. *Chem. Rev.* **1989**, *89*, 1875. (b) Hay, B. P.; Rustad, J. R. *J. Am. Chem. Soc.* **1994**, *116*, 6316. (c) Hay, B. P. *Coord. Chem. Rev.* **1993**, *126*, 177. (d) Martell, A. E.; Hancock, R. D.; Motekaitis, R. J. *Coord. Chem. Rev.* **1994**, *133*, 39. (e) Dishong, D. M.; Gokel, G. W. *J. Org. Chem.* **1982**, *47*, 147.
(10) (a) Beer, P. D. *Chem. Soc. Rev.* **1989**, *18*, 409. (b) Beer, P. D. *Adv. Inorg. Chem.* **1992**, *36*, 79.
(11) (a) Massaux, J.; Desreux, J. F.; Duyckaerts, G. *J. Chem. Soc., Dalton Trans.* **1980**, 865. (b) Quici, S.; Anelli, P. L.; Molinari, H.; Beringhelli, T. *Pure Appl. Chem.* **1986**, *58*, 1503. (c) Cheney, J.; Kintzinger, J. P.; Lehn, J. M. *Nouv. J. Chim.* **1978**, *2*, 411.
(12) Plenio, H.; El-Desoky, H.; Heinze, J. *Chem. Ber.* **1993**, *126*, 2403.
(13) (a) vanVeggel, F. C. J. M.; Verboom, W.; Reinhoudt, D. N. *Chem. Rev.* **1994**, *94*, 279. (b) Beer, P. D. *Adv. Inorg. Chem.* **1992**, *39*, 79.
(14) Medina, J. C.; Goodnow, T. T.; Rojas, M. T.; Atwood, J. L.; Lynn, B. C.; Kaifer, A. E.; Gokel, G. W. *J. Am. Chem. Soc.* **1992**, *114*, 10583.
(15) Tverdokhlebov, V. P.; Tselinskii, I. V.; Gidaspov, B. V.; Chikisheva, G. Y. *J. Org. Chem. (USSR) (Engl. Transl.)* **1976**, *12*, 2268.
(16) (a) Calverly, M. J.; Dale, J. *J. Chem. Soc., Chem. Commun.* **1981**, 684. (b) Calverly, M. J.; Dale, J. *J. Chem. Soc., Chem. Commun.* **1981**, 1084.
(17) El-Amin, B.; Anantharamaiah, D. M.; Royer, G. P., Means, G. G. *J. Org. Chem.* **1979**, *44*, 3442.
(18) (a) Copland, M. A.; Fuoss, R. M. *J. Phys. Chem.* **1964**, *68*, 1177. (b) Brown, R.; Jones, W. E. *J. Chem. Soc.* **1946**, 781.
(19) Moore, S. S.; Tarnowski, T. L.; Newcomb, M.; Cram, D. J. *J. Am. Chem. Soc.* **1977**, *99*, 6398.
(20) Sheldrick, G. M. SHELXS-86, SHELXL-93, Universität Göttingen, 1986, 1993.

Table 1. Crystal Data Summary

	3	**4**	**3**·2HClO$_4$	[(**2**)NaClO$_4$]$_2$	(**4**)NaI
empirical formula	$C_{40}H_{56}Fe_2N_4O_4$	$C_{30}H_{48}FeN_4O_4$	$C_{44}H_{64}Cl_2Fe_2N_6O_{12}$	$C_{28}H_{44}ClFeN_2NaO_{11}$	$C_{30}H_{48}FeIN_4NaO_4$
fw	768.59	584.58	1051.61	698.94	734.48
temp (K)	293(2)	293(2)	293(2)	293	213(2)
wavelength (pm)	71.069	71.069	71.069	71.069	71.069
cryst syst	triclinic	triclinic	monoclinic	tetragonal	orthorhombic
space group	$P\bar{1}$	$P\bar{1}$	$P2_1/c$	$I4_1/acd$	$Pbca$
unit cell					
a (pm)	1191.8(2)	1239.9(1)	1094.6(2)	2876.6(4)	1687.2(3)
b (pm)	1273.5(3)	1297.9(1)	2319.1(5)	2876.6(4)	1308.8(3)
c (pm)	1398.1(3)	1971.0(2)	978.3(2)	1626.9(3)	2925.0(6)
α (deg)	67.00(3)	107.60(1)	90	90	90
β (deg)	83.89(3)	96.34(1)	103.53(3)	90	90
γ (deg)	69.18(3)	95.61(1)	90	90	90
vol (Å^3)	1824.4(7)	2976.0(4)	2414.5(8)	13462(4)	6459(2)
Z	2	4	2	16	8
density (g cm^{-3})	1.399	1.305	1.446	1.379	1.510
abs (mm^{-1})	0.842	0.547	0.778	0.60	1.48
F(000)	816	1256	1104	5888	3024
θ range (deg)	2.9−26.0	2.3−26.0	2.3−23.3	2.7−23.2	3.6−22.5
Index range (h,k,l)	14/14,−14/15,0/17	−15/15,−15/15,−14/0	−12/0,−25/0,−10/10	−31/0,−31/0,−17/0	−8/18,0/14,−31/31
no of reflcns collcd	7489	11995	3325	4716	4273
no of indep reflcns	7172	11639	3153	2401	4161
data/param	6084/451	11610/703	2385/299	1755/222	3755/383
GooF	1.08	1.13	1.07	1.08	1.06
R index ($2\sigma(I)$)					
R1	6.07	5.63	5.28	7.21	5.14
wR2	15.96	12.97	12.09	18.86	11.24
largest peak (e Å^{-3})	+0.85	+0.89	+0.55	+0.46	+0.63
largest hole (e Å^{-3})	−1.01	−0.41	−0.36	−0.29	−1.01

Table 2. Selected Atomic Coordinates ($\times 10^4$) for **3**[a]

	x	y	z
Fe(1)	1680(1)	5719(1)	5628(1)
C(1)	2670(4)	3906(4)	6433(3)
C(2)	2332(4)	4553(4)	7103(3)
C(3)	1047(4)	5047(4)	7065(3)
C(4)	605(4)	4730(4)	6356(3)
C(5)	1615(4)	4027(4)	5970(3)
C(6)	845(4)	7568(4)	5077(3)
C(7)	710(4)	7114(4)	4337(3)
C(8)	1869(4)	6512(4)	4066(4)
C(9)	2722(5)	6594(5)	4630(4)
C(10)	2098(4)	7252(4)	5249(4)
C(11)	3934(4)	3107(4)	6367(3)
N(1)	4057(3)	2544(3)	5607(3)
C(12)	5019(4)	1356(4)	5918(3)
C(13)	4618(4)	346(4)	6670(3)
O(1)	3766(3)	125(3)	6194(3)
C(14)	4176(4)	3361(4)	4559(3)
C(15)	3852(4)	3030(4)	3736(3)
O(2)	2594(3)	3314(3)	3690(2)
C(16)	−174(4)	8281(4)	5568(4)
N(2)	−1346(3)	8474(3)	5173(3)
C(17)	−1693(4)	9480(4)	4163(4)
C(18)	−2560(4)	9386(4)	3517(3)
C(19)	−2275(4)	8602(4)	5935(3)
C(20)	−2244(4)	7375(4)	6740(3)

[a] Symmetry operation used to generate equiv atoms: $-x$, $1-y$, $1-z$.

under their CSD-depository numbers. Definition of R values: $R1 = \sum|F_o - F_c| / \sum(F_o)$; $wR2 = [\sum[w(F_o^2 - F_c^2)^2] / \sum[w(F_o^2)^2]]^{0.5}$; GooF = $[\sum[w(F_o^2 - F_c^2)^2] / (n-p)]^{0.5}$.

[(2)NaBPh$_4$]$_2$. The structure was solved using direct methods and refined by full-matrix least-squares against F^2. Anisotropic parameters were used for most atoms except several carbon and oxygen atoms within the 12-membered rings. Due to the poor quality of the crystal structure the data were not deposited. Abbreviated crystal data: $C_{52}H_{64}BFeN_2NaO_6$ (902.74); $R\bar{3}$, a = 4579.3(6) pm, V = 52301(15) Å^3; Cu Kα, Z = 45; collected (independent) data 29 046 (9401), data/parameter = 7936/1166; $R1$ = 11.5, $wR2$ = 30.96, largest peak and hole = +0.97, −3.53. Single crystals were grown by slowly cooling a toluene solution.

[(2)NaClO$_4$]$_2$. The structure was solved using direct methods and refined by full-matrix least-squares against F^2. Anisotropic thermal parameters were used for all non-hydrogen atoms; hydrogen atom parameters followed a riding model. Single crystals were grown by allowing ether to slowly diffuse into an acetonitrile solution. Depository number: CSD-401600.

3. The structure was solved by direct methods and refined by full-matrix least-squares against F^2. The unit cell contains two slightly different molecules which both have a crystallographic inversion center. Anisotropic thermal parameters for all non-hydrogen atoms; hydrogen atoms (riding model). Single crystals were grown by slowly cooling an ethanol solution. CSD-401119.

3·2HClO$_4$. The structure was solved using direct methods and refined by full-matrix least-squares against F^2. Anisotropic thermal parameters were used for all non-hydrogen atoms; hydrogen atoms parameters followed a riding model. The N−H proton was localized on the final difference Fourier map (N(1)−H, 89 pm). Single crystals were grown by allowing ether to slowly diffuse into an acetonitrile solution. Depository number: CSD-400747.

4. The structure was solved by a combination of heavy atom and Patterson techniques and refined by full-matrix least-squares against F^2. The unit cell contains two different molecules. Anisotropic thermal parameters were used for all non-hydrogen atoms; hydrogen atom parameters followed a riding model. Single crystals were grown by slowly cooling a pentane solution. Depository number: CSD-401120.

(4)NaI. The structure was solved by a combination of Patterson and Fourier techniques and refined by full-matrix least-squares against F^2. Anisotropic thermal parameters were used for all non-hydrogen atoms; hydrogen atom parameters followed a riding model. Single crystals were grown by allowing ether to slowly diffuse into an acetonitrile solution. Depository number: CSD-401118.

Results and Discussion

The ferrocene crown ethers were synthesized using [1,1′-ferrocenediylbis(methylene)]bis[pyridinium]tosylate chloride (**1**) as a starting material, which is easily available from ferrocene in two steps[15] The reaction of **1** with aza-12-crown-4 [H(N-12-C-4)], diaza-12-crown-4 [H(N$_2$-12-C-4)H], or 1,2-ethanediyl-bis(1,7-dioxa-4,10-diazacyclododecane) [C$_2$H$_4$diyl-((N$_2$-12-C-4)H)$_2$] yields the ferrocene macrocycles 1,1′-ferrocenediylbis(10-methylene-1,4,7-trioxa-10-azacyclododecane) [Fcdiyl(N-12-C-

Table 3. Atomic Coordinates ($\times 10^4$) for **4**

	x	*y*	*z*
Fe(1)	902(1)	2749(1)	1002(1)
C(1)	−694(3)	3029(3)	950(2)
C(2)	−195(4)	3314(4)	401(2)
C(3)	709(4)	4127(4)	738(3)
C(4)	784(4)	4345(3)	1488(3)
C(5)	−90(3)	3680(3)	1620(2)
C(6)	2259(3)	2165(3)	600(2)
C(7)	2397(3)	2426(4)	1362(2)
C(8)	1553(4)	1800(4)	1546(3)
C(9)	883(4)	1147(3)	911(3)
C(10)	1314(3)	1370(3)	322(2)
C(11)	−1686(3)	2204(4)	841(3)
N(1)	−2643(3)	2362(3)	402(2)
C(12)	−2957(4)	3447(4)	617(2)
C(13)	−3591(4)	3724(4)	2(2)
O(1)	−2936(3)	4057(3)	−451(2)
C(14)	−2640(4)	3181(4)	−996(3)
C(15)	−3558(4)	2733(4)	−1645(3)
N(2)	−3339(3)	1714(3)	−2106(2)
C(16)	−4069(5)	746(4)	−2194(3)
C(17)	−3832(5)	197(4)	−1644(3)
O(2)	−3982(2)	902(3)	−960(2)
C(18)	−3597(4)	562(4)	−373(3)
C(19)	−3553(3)	1500(4)	304(3)
C(20)	3010(3)	2635(4)	186(2)
N(3)	2727(3)	2171(3)	−595(2)
C(21)	2980(4)	1053(3)	−862(2)
C(22)	2365(4)	414(4)	−1591(2)
O(3)	1234(3)	149(3)	−1573(2)
C(23)	511(5)	530(5)	−2061(3)
C(24)	−119(5)	1298(4)	−1620(3)
N(4)	−798(3)	1865(3)	−2045(2)
C(25)	−197(4)	2678(4)	−2285(2)
C(26)	665(4)	3454(4)	−1729(3)
O(4)	1626(2)	2958(2)	−1687(2)
C(27)	2470(4)	3617(3)	−1140(2)
C(28)	3239(3)	2880(4)	−955(3)
C(29)	−2692(4)	1715(4)	−2670(3)
C(30)	−1658(4)	1193(4)	−2616(3)
Fe(2)	7969(1)	4309(1)	5863(1)
C(101)	7570(3)	5831(3)	5945(2)
C(102)	7610(4)	5641(4)	6619(2)
C(103)	6855(4)	4719(4)	6544(3)
C(104)	6328(4)	4318(4)	5827(3)
C(105)	6759(3)	5000(4)	5460(2)
C(106)	8269(3)	2842(3)	5198(2)
C(107)	8587(3)	2931(3)	5930(2)
C(108)	9386(3)	3867(3)	6245(2)
C(109)	9560(3)	4359(3)	5708(2)
C(110)	8876(3)	3725(3)	5068(2)
C(111)	8298(3)	6669(3)	5765(3)
N(101)	7866(3)	7712(3)	5850(2)
C(112)	8737(4)	8567(3)	5855(3)
C(113)	9214(4)	8490(4)	5176(3)
O(101)	8513(2)	8899(2)	4732(2)
C(114)	8614(4)	8557(4)	3991(3)
C(115)	7534(4)	8595(4)	3586(3)
N(102)	6685(3)	7745(3)	3601(2)
C(116)	5600(4)	8087(4)	3616(3)
C(117)	5417(4)	8845(4)	4328(3)
O(102)	5405(2)	8356(3)	4880(2)
C(118)	6387(3)	8594(3)	5378(2)
C(119)	6905(3)	7560(3)	5310(2)
C(120)	7463(3)	1938(3)	4670(2)
N(103)	7285(2)	2041(3)	3949(2)
C(121)	8219(3)	1795(3)	3561(2)
C(122)	8297(4)	2329(3)	2977(2)
O(103)	8648(2)	3479(2)	3258(2)
C(123)	7783(3)	4140(3)	3343(2)
C(124)	7336(3)	4282(4)	2631(2)
N(104)	6308(3)	4741(3)	2597(2)
C(125)	5308(4)	3973(4)	2383(3)
C(126)	4950(4)	3427(4)	2916(3)
O(104)	5618(2)	2611(2)	2940(2)
C(127)	5387(3)	2114(3)	3464(2)
C(128)	6243(3)	1397(3)	3532(2)
C(129)	6704(4)	6735(4)	3014(2)
C(130)	6239(4)	5740(4)	3173(3)

Table 4. Selected (Cationic Part) Atomic Coordinates ($\times 10^4$) for **3**·2HClO$_4$[a]

	x	*y*	*z*
Fe	3979(1)	1665(1)	2065(1)
C(1)	2117(6)	1791(4)	1963(9)
C(2)	2537(7)	2169(3)	1038(9)
C(3)	2996(7)	1841(3)	56(7)
C(4)	2875(5)	1250(3)	359(7)
C(5)	2319(6)	1226(3)	1551(7)
C(6)	5834(6)	1759(3)	2114(8)
C(7)	5435(7)	2198(3)	2895(10)
C(8)	4966(7)	1947(4)	3977(8)
C(9)	5089(6)	1351(3)	3896(7)
C(10)	5619(5)	1220(3)	2734(6)
C(11)	5935(5)	634(3)	2310(6)
N(1)	7289(4)	473(2)	2949(5)
C(12)	8142(6)	844(3)	2334(8)
C(13)	7634(6)	463(3)	4508(6)
O(1)	9780(4)	113(2)	3010(5)
C(14)	9513(6)	706(3)	2848(9)
C(15)	6828(7)	52(3)	5101(8)
O(2)	6503(4)	−443(2)	4266(5)
C(16)	3132(6)	748(3)	−476(6)
N(2)	2309(4)	703(2)	−1909(5)
C(17)	968(6)	764(3)	−1942(8)
C(18)	2679(7)	1124(3)	−2914(7)
C(19)	2523(7)	854(3)	−4343(7)
C(20)	9638(6)	−206(3)	1734(7)

[a] Symmetry operations used to generate equiv atoms: $1 - x, -y, -z$.

Table 5. Selected (Cationic Part) Atomic Coordinates ($\times 10^4$) for [(**2**)NaClO$_4$]$_2$

	x	*y*	*z*
Fe(1)	907(1)	1593(1)	1250
C(1)	561(4)	1817(3)	237(4)
C(2)	1034(4)	1740(5)	44(5)
C(3)	1127(3)	1264(5)	222(6)
C(4)	714(3)	1054(3)	514(5)
C(5)	365(3)	1398(3)	538(4)
C(6)	−112(3)	1342(3)	888(5)
N(1)	−488(2)	1249(3)	303(4)
C(7)	−431(4)	837(5)	−168(8)
C(8)	−561(5)	427(4)	257(8)
O(1)	−1051(3)	420(2)	546(4)
C(9)	−1357(5)	256(4)	−43(9)
C(10)	−1801(4)	394(5)	129(10)
O(2)	−1870(2)	907(3)	248(5)
C(11)	−1936(5)	1163(7)	−475(8)
C(12)	−1846(4)	1626(4)	−283(7)
O(3)	−1359(2)	1715(2)	21(3)
C(13)	−1037(4)	1713(5)	−584(7)
C(14)	−579(4)	1689(4)	−236(6)
Na(1)	−1290(1)	1210(1)	1250

4)$_2$] (**2**),[12] 1,1″:1′,1‴-bis(ferrocenediyl)bis[4,10-bis(methylene)-1,7-dioxa-4,10-diazacyclododecane] [Fcdiyl(N$_2$-12-C-4)$_2$Fcdiyl] (**3**), and 1,1′-ferrocenediyl-10,10′-(1,2-ethanediyl)bis[4-methylene-1,7-dioxa-4,10-diazacyclododecane] [Fcdiyl(N$_2$-12-C-4)$_2$-(C$_2$H$_4$)diyl] (**4**) in yields of 55%, 10%, and 24%, respectively (Scheme 1).[21]

For the synthesis of **4** the choice of the right metal template is important since only in the presence of Li_2CO_3 are significant amounts of **4** produced. With other bases such as Na_2CO_3 or K_2CO_3 no product could be isolated.

In the NMR spectra of **2**, **3**, and **4** complex formation with Li^+, Na^+, and K^+ is evidenced, by shifts of the NMR signals. The addition of lithium and sodium salts to solutions of **2** and **3** in acetonitrile continuously shifts the resonance positions until the final value corresponding to the metal complex (complexes of **3** are weak) is reached (fast exchange), whereas in the case of **4** the NMR spectra of the Li^+, Na^+, and K^+ complexes are

(21) Instead of the extremely long IUPAC names short forms are used here. Fcdiyl stands for 1,1′-ferrocenediylbis(methylene), H(N$_2$-12-C-4)H for the free crown ether, and (N$_2$-12-C-4) for the doubly deprotonated bridge in the ferrocene crown ethers.

Table 6. Atomic Coordinates ($\times 10^4$) for (**4**)NaI

	x	*y*	*z*
I(1)	594(1)	2227(1)	6167(1)
Na(1)	−705(1)	2832(2)	4050(1)
Fe(1)	1870(1)	−20(1)	3444(1)
C(1)	1514(4)	844(7)	3988(2)
C(2)	1555(5)	−207(8)	4112(2)
C(3)	2342(6)	−553(10)	4032(3)
C(4)	2800(6)	260(11)	3881(4)
C(5)	2293(4)	1136(8)	3853(3)
C(6)	1351(4)	499(6)	2845(2)
C(7)	912(4)	−307(7)	3042(3)
C(8)	1384(5)	−1197(7)	3085(3)
C(9)	2141(5)	−926(7)	2905(3)
C(10)	2122(4)	91(7)	2765(3)
C(11)	811(4)	1547(6)	3969(2)
N(1)	265(3)	1584(4)	4360(2)
C(12)	647(4)	1929(5)	4780(2)
C(13)	766(4)	3082(5)	4776(2)
O(1)	51(2)	3636(3)	4698(1)
C(14)	−419(4)	3771(5)	5103(2)
C(15)	−1210(4)	4202(5)	4953(2)
N(2)	−1660(3)	3505(4)	4656(2)
C(16)	−1992(4)	2652(5)	4917(2)
C(17)	−2159(4)	1742(5)	4621(3)
O(2)	−1465(2)	1389(3)	4387(2)
C(18)	−958(4)	784(5)	4669(3)
C(19)	−179(4)	622(5)	4421(3)
C(20)	1097(4)	1553(6)	2698(3)
N(3)	344(3)	1945(5)	2876(2)
C(21)	308(5)	3067(6)	2787(3)
C(22)	670(4)	3681(6)	3162(3)
O(3)	173(2)	3845(3)	3555(1)
C(23)	−266(4)	4792(5)	3562(2)
C(24)	−1084(4)	4691(5)	3359(2)
C(25)	−2200(4)	3490(6)	3383(2)
N(4)	−1605(3)	4042(4)	3652(2)
C(26)	−1908(5)	2557(7)	3159(4)
O(4A)	−1296(5)	2054(7)	3339(3)
O(4B)	−1271(7)	2439(11)	2989(5)
C(27A)	−1026(7)	1116(11)	3108(5)
C(27B)	−991(15)	1460(19)	2892(8)
C(28)	−361(5)	1413(7)	2682(3)
C(29)	−2285(4)	4052(5)	4405(2)
C(30)	−1982(4)	4679(5)	4008(2)

Scheme 1. Synthesis of the Ferrocene Crown Ethers[a]

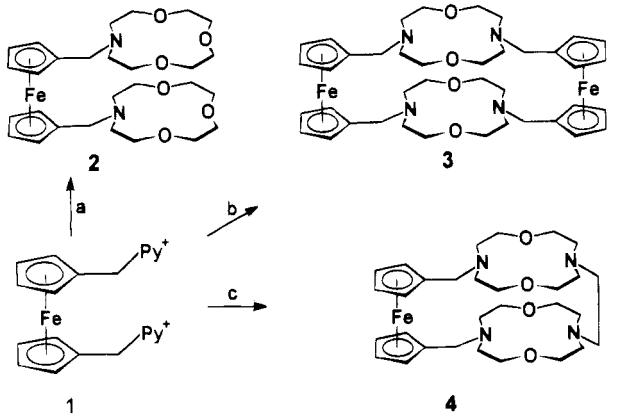

[a] Key: (a) H(N-12-C-4), Na_2CO_3; (b) H(N_2-12-C-4)H, Na_2CO_3; (c) C_2H_4diyl(HN_2-12-C-4)$_2$, Li_2CO_3.

in the slow-exchange region, reflecting the better preorganization of the donor atoms. Addition of substoichiometric amounts of metal ions immediately gives rise to a new set of resonances corresponding to metal complexes of **4**.

Metal Ion Selectivities. Picrate extraction experiments were performed to determine metal ion selectivities. Ferrocene crown **2** displays some selectivity toward complexation of Li^+, (**2**)Li^+ (log K_a = 6.0) (**2**)Na^+ (log K_a = 5.1), and (**2**)K^+ (log K_a = 5.0). Much stronger complexes are formed by **4** since this ligand is much better preorganized to accommodate metal ions. The association constants reveal significant differences between the metal ions (**4**)Li^+ (log K_a = 8.0), (**4**)Na^+ (log K_a = 6.6), and (**4**)K^+ (log K_a = 6.3). The strongest complexes of **4** are, somewhat unexpectedly, formed with Li^+ which also explains why using Li_2CO_3 as a templating base in the synthesis of **4** gave the best yields. This can be rationalized by taking a closer look at the crystal structure of (**4**)NaI, since the ligand cannot provide enough donor atoms for Na^+ (see solid-state structure, Figure 6). The selectivities for the complexation of the smaller cations by **4** are even more significant, since the differentiation between potassium and the smaller ions is usually less well pronounced in the picrate experiments. The heterogenous stability constant K_a describes the distribution between an aqueous layer and a much less polar organic solvent ($CHCl_3$) and is influenced by the fact that smaller ions possess a much more strongly bound hydration shell.[3]

We have therefore also performed NMR experiments and FAB mass spectrometry (see also Cyclic Voltammetry) to better understand the metal ion selectivity diplayed by **4**. NMR spectroscopy is only useful when the selectivities are smaller than approximately 50, which was indicated by the picrate extraction experiments. However, in the NMR spectra (^1H, ^{13}C) of equimolar mixtures of **4**, $NaClO_4$, and $KClO_4$ in CD_3CN, the intensity ratio of the NMR signals of (**4**)Na^+ and (**4**)K^+ was observed with a selectivity of ca. 25:1.[22] To probe the selectivity of crown ethers FAB-MS is a useful semiquantitative technique.[23] As can be seen in the FAB-MS (Figure 1), the ferrocene crown **4** displays a good selectivity for Na^+ vs K^+ complexation. The relative intensities of the signals of the metal complexes with **4** [(**4**)H^+ (*m/e* = 585)] are a measure of the selectivity and show (**4**)Na^+ (*m/e* = 607) has a substantially higher ion count rate than (**4**)K^+ (*m/e* = 624), whereas the preference for Li^+ is not obvious in the FAB-MS. From these measurements was calculated an approximate Na^+ vs K^+ selectivity for **4** of 50:1. Selectivity for the complexation of Na^+ vs K^+ is much more pronounced in the NMR and the FAB-MS experiments and demonstrates the influence of different techniques and different experimental conditions used to obtain the relative stability constants.

Cyclic Voltammetry. Since the ferrocene crown ether **4** displays good Li^+ vs Na^+ and Na^+ vs K^+ selectivities, it was of interest to see if it was possible to recognize metal ions electrochemically. Whereas **2** is oxidized reversibly at $E_{1/2}$ = +0.35 V (vs cobaltocene $E_{1/2}$ = −0.94 V vs Ag/AgCl), this process is not reversible for the free ferrocene crown ethers **3** and **4** at room temperature. In CH_3CN and other solvents the oxidation of these ligands results in a complex sequence of irreversible electron transfer processes. This behavior was unexpected since none of the related ferrocene crowns with 15- or 18-membered rings display irreversible redox processes. Performing the cyclic voltammetry of **3** and **4** in CH_3CN at −30 °C, resulted in a reversible oxidation of **4** with $E_{1/2}$ = +0.27 V. Upon addition of $LiClO_4$ or $NaClO_4$ to CH_3CN solutions of **2** or **4** the redox potentials are shifted to anodic values by +100 mV (**2** + Li^+), +70 mV (**2** + Na^+), +140 mV (**4** + Li^+), and +100 mV (**4** + Na^+), whereas $KClO_4$ did not produce any effect. Incorporation of metal ions into the cavity of **4** gives fully reversible cyclic voltammograms of (**4**)Li^+ and (**4**)Na^+ at room temperature, whereas there is no change toward revers-

(22) Analogous experiments could not be performed with lithium complexes since the ^1H NMR resonances are overlapping and the ^{13}C NMR lines are exchange broadened between 270 and 330 K.

(23) (a) Johnstone, R. A. W.; Rose, M. E. *J. Chem. Soc., Chem. Commun.* **1983**, 1268. (b) Takahashi, T.; Uchiyama, K.; Yamada, K.; Lynn, B. C.; Gokel, G. W. *Tetrahedron Lett.* **1992**, 3825. (c) Beer, P. D.; Tite, E. L.; Ibbotson, A. *J. Chem. Soc., Dalton Trans.* **1990**, 2691.

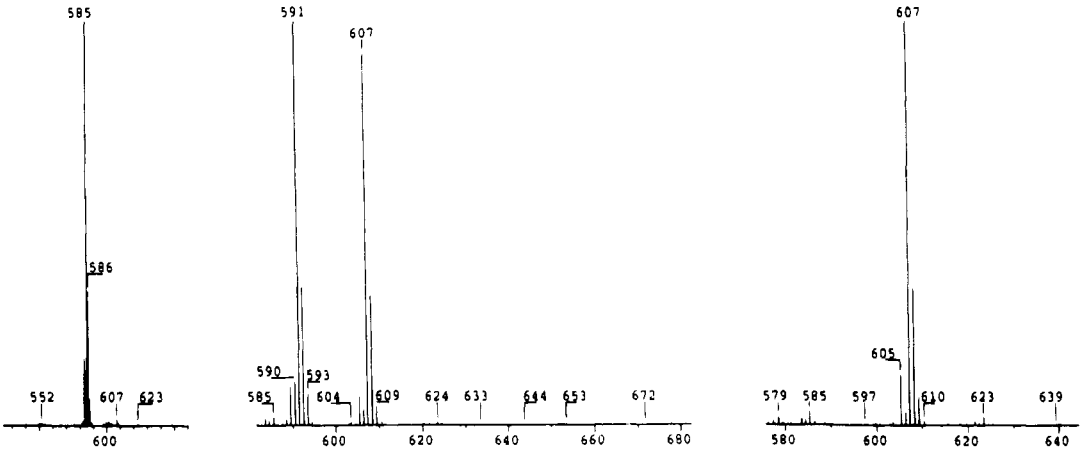

Figure 1. FAB-MS of (left) **4**, *m/e* = 585 ((**4**)H$^+$) (middle) **4** + (Li, Na, K, Rb)ClO_4, *m/e* = 591 ((**4**)Li$^+$), 607 ((**4**)Na$^+$), and (right) **4** + (Na, K, Rb)ClO_4, *m/e* = 624 ((**4**)K$^+$).

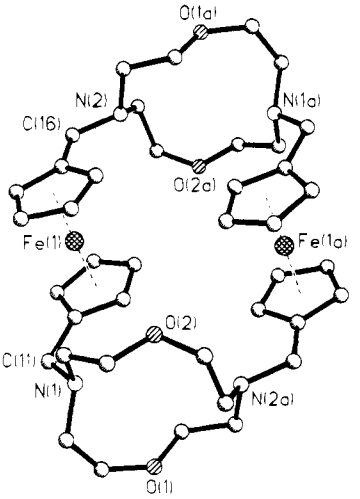

Figure 2. Molecular structure of **3** (without hydrogen atoms). Selected interatomic distances (pm): N(1)−O(1), 300.1; N(1)−O(2), 298.5; N(2a)−O(1), 316.3; N(2a)−O(2), 300.0; Fe(1)−Fe(1a), 563.0; N(1)−N(2a), 426.0.

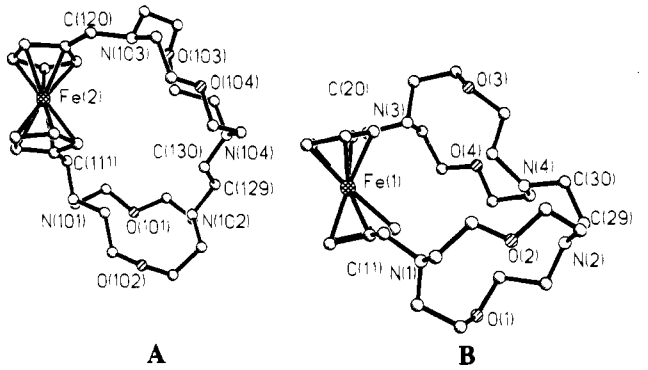

Figure 3. Molecular structure of **4** (without hydrogen atoms): molecule A, Fe(1); molecule B, Fe(2). Selected bond angles (deg): N(2)−C(29)−C(30)−N(4), 74.1; N(102)−C(129)−C(130)−N(104), 177.5; Cp−Cp′ (A), 1.5; Cp−Cp′ (B), 2.6.

ibility in **3** even upon addition of metal salts. The anodic shift of the redox potentials of the complexes of **4** with Li$^+$ or Na$^+$ is too small to switch the bonding of the metal ions within the macrocycle. However, the highly selective coordination of Li$^+$ vs Na$^+$ or Li$^+$ vs K$^+$ can be used to electrochemically detect Li$^+$ even in the presence of a large excess of potassium or sodium ions thus making compound **4** a prototype amperometric Li$^+$ sensor.[24] The same holds true for Na$^+$, because it could be detected electrochemically even in the presence of excess K$^+$.

Solid-State Structures of 3, 4, 3·2HClO$_4$, [(2)NaBPh$_4$)$_2$, [(2)NaClO$_4$)$_2$, and (4)NaI. In the solid-state structures of each of the free ligands **3** (Figure 2, Table 2) and **4** (Figure 3, Table 3), two independent molecules are found in the unit cell. This obviously is a result of the conformative flexibility of the 12-membered crown ether rings.[25] In **3** the two molecules differ only slightly with respect to the orientation of the crown ether rings and will therefore not be discussed separately. In **4** the two molecules **4a** and **4b** are quite different, the most obvious difference being the orientation of the substituents at the C_2H_4 unit bridging the two 12-membered rings. In **4a** the torsion angle N(2)−C(29)−C(30)−N(4) is 74.1°, and in **4b** it is 177.5°. It seems to be typical of free ferrocene cryptands (in the solid-state) that the nitrogen atoms have their lone pairs oriented toward the inside of the cavity and/or that the nitrogen atoms lie in a plane with the cyclopentadienyl rings. This holds true in the structure of **3** and for six of the eight nitrogen atoms in the two independent molecules of **4**, even though N(2) is almost in a trigonal planar environment (angles around N(2) = 119.0, 119.0, and 117.6°).

It is interesting to observe how the addition of two protons to **3** to give **3**·2 HClO$_4$ (Figure 4, Table 4) changes this flexible arrangement of the atoms. In the solid-state structure of **3**·2HClO$_4$ the two 12-membered macrocycles are folded such that pairs of nitrogens in the same ring have a distance of only 297.9 pm, whereas the average value in **3** is 425.9 pm.[26] This is larger than the maximum for a symmetrical N−H−N$^+$ bridge (280 pm)[27] with the internitrogen distance being intermediate to those of the related monoprotonated cryptand [1.1.1][28] and 1,6-diazabicyclo[4.4.4]tetradecane salts.[29] The asymmetric NH bonding in **3**·2HClO$_4$ is not reflected in the geometry of the nitrogen atoms, as the bond angles and distances of N(1) and N(2) to the adjacent carbon atoms are quite similar (109.6−114.7°, 146.8−151.5 pm). However, there is a significant difference of the contact distances between the nitrogen and the oxygen atoms of N(1)−O(1) (283.9 pm), N(1)−O(2) (272.6 pm) and N(2)−O(1a) (297.1 pm), N(2)−O(2a) (296.2 pm). The

(24) (a) Beer, P. D.; Danks, J. P.; Drew, M. G. B.; McAleer, J. F. *J. Organomet. Chem.* **1994**, *476*, 63. (b) Scholl, A. F.; Sutherland, I. O. *J. Chem. Soc., Chem. Commun.* **1992**, 1716.
(25) Goldberg, S. In *Crown Ethers and Analogs*; Patai, S., Rappoport, Z., Eds.; J. Wiley: Chichester, U.K., 1989.
(26) Geue, R.; Jacobson, S. H.; Pizer, R. *J. Am. Chem. Soc.* **1986**, *108*, 1150.
(27) Alder, R. W. *Tetrahedron* **1990**, *46*, 683.
(28) Brügge, H. J.; D. Carboo, D.; vonDeuten, K.; Knöchel, A.; Kopf, J.; Dreissig, W. *J. Am. Chem. Soc.* **1986**, *108*, 107.
(29) Alder, R. W.; Orpen, A. G.; Sessions, R. B. *J. Chem. Soc., Chem. Commun.* **1983**, 999.

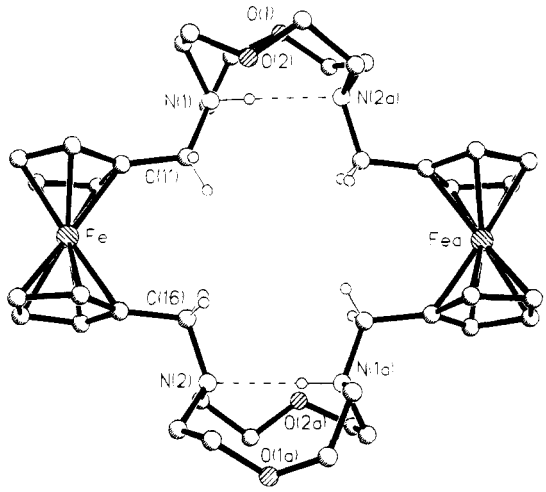

Figure 4. Molecular structure of **3**·2HClO$_4$ (most hydrogen atoms omitted). Selected interatomic distances (pm) and angles (deg): Fe(1)–Fe(1a), 923.0; N(1)–O(1), 283.9; N(1)–O(2), 272.6; N(2)–O(1a), 297.1; N(2)–O(2a), 296.2; Cp–Cp′, 2.1.

much closer oxygen distances to N(1) in the protonated species could be due to a partial stabilization of the excess charge by additional oxgen–proton contacts and suggest a position of the proton close to N(1), where it was localized on the final difference Fourier map. Another difference between the structures of **3** and **3**·2HClO$_4$ is the change of the orientation of the vectors C(11)–N(1) and C(16)–N(2) with respect to the planes of the respective cyclopentadienyl rings. Prior to protonation N(1) and N(2) are located almost within the plane of the ring, whereas in **3**·2HClO$_4$ the angles of the carbon–nitrogen vectors with the plane of the respective cyclopentadienyl ring are close to their maximum possible value, resulting in much larger Fe–N distances. Another consequence of protonation as well as of metal coordination is that the vectors from the centroids of the cyclopentadienyl rings to C(11) and C(16), respectively, are almost in a parallel alignment [**3**·2HClO$_4$, [Cent.–C(11)]–[Cent.–C(16)] = 14.0°; (**4**)NaI, [Cent.–C(11)]–[Cent.–C(20)] = 17.3°] but not so in the free ligands [**3**, [Cent.–C(11)]–[Cent.–C(16)] = 150.9°; **4A**, [Cent.–C(11)]–[Cent.–C(20)] = 133.5°; **4B**, [Cent.–C(111)]–[Cent.–C(120)] = 118.5°].

In order to maximize the interaction of the donor atoms with the Lewis acids within the cavity, these two types of conformational changes occur, since only then all donor atoms can participate equally in the bonding of the proton or the metal ion. This explains why the sandwiching of a metal ion between two crown ether units bonded to the same ferrocene unit is difficult, as long as 1,1′-ferrocenediylbis(methylene) groups are bridging the two crown ether rings. As can be seen easily in the structure of **3**·2HClO$_4$ the hydrogen atoms attached to C(11) and C(16) would get into the way of the metal ion. This explains why it was not possible to isolate a complex of **3** with a metal ion encapsulated between the two 12-membered crowns (even though some kind of side-on sandwich complex appears possible[30]). However, since the sandwiching of Na^+ between two 12-membered crown ethers is highly favored, a dimeric complex is formed with ferrocene crown ether **2** and NaClO$_4$ as well as in **2** and NaBPh$_4$.

In [(**2**)NaClO$_4$]$_2$ (Figure 5, Table 5) each of the 12-membered crown ether rings connected to one ferrocene group coordinates to a different Na^+. This dimerization allows a maximum angle

(30) Otherwise it would be difficult to understand why the NMR spectra are indicative of complex formation with Na^+, whereas in the solid-state structure of **3** and **3**·2HClO$_4$ it is not clear how the metal ion can be coordinated.

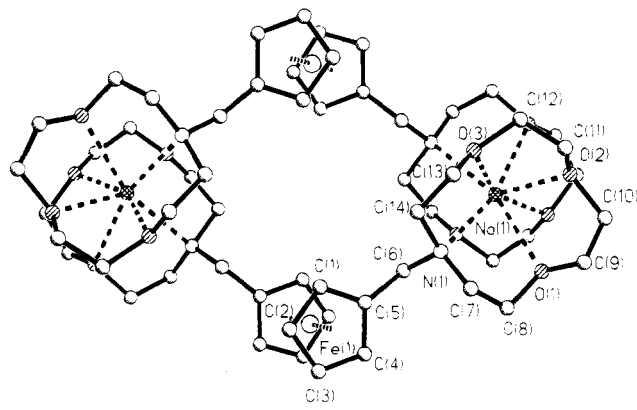

Figure 5. Molecular structure of [(**2**)NaClO$_4$]$_2$ (without hydrogen atoms). Selected bond lengths (pm), interatomic distances (pm), and interplanar angles (deg): Na(1)–O(1), 263.6(7); Na(1)–O(2), 249.0(8); Na(1)–O(3), 248.0(6); Na(1)–N(1), 277.5(7); Fe(1)–Fe(1a), 737.6; Na(1)–Na(1a), 1049.5; Fe(1)–Na(1), 641.4; Cp–Cp′, 1.3.

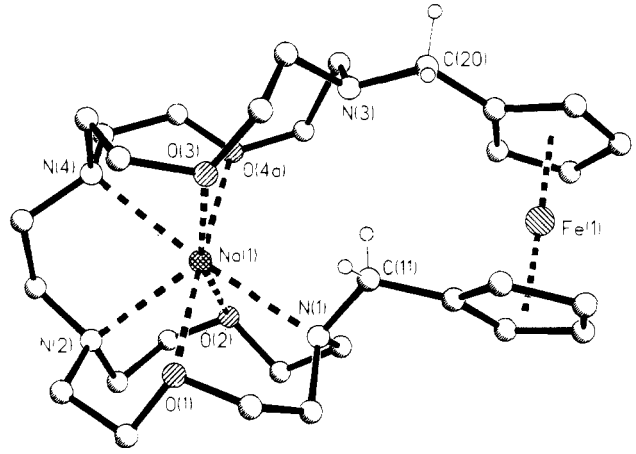

Figure 6. Molecular structure of (**4**)NaI (most hydrogen atoms omitted). Selected interatomic distances (pm), bond lengths (pm), and angles (deg): Fe(1)–Na(1), 599.6; Na(1)–O(3), 246.0(5); Na(1)–N(1), 248.3(5); Na(1)–N(4), 248.3(6); Na(1)–O(2), 248.6(5); Na(1)–O(4a), 252.2(9); Na(1)–N(2), 255.3(5); Cp–Cp′, 5.0.

of the Fc**C**H$_2$–**N** vectors with respect to the plane of the respective cyclopentadienyl ring. The Na^+–O (248.0(6), 249.0(8), 263.6(7) pm in [(**2**)NaClO$_4$]$_2$ and 246–259 pm in [(**2**)-NaBPh$_4$]$_2$) bond lengths are comparable to those of the two sandwich complexes of 12-C-4 with Na^+ described by vanRemoortere and Boer (average Na^+–O = 249.7 and 248.5 pm)[31] and that of Na^+ with two aza-12-C-4 by Gokel et al.[32] It is of significance for the following discussion of the electrochemistry of the ferrocene crown ether complexes that the Fe–Na^+ distances of 641.4 pm and 650 pm (average of two distances) in [(**2**)NaClO$_4$]$_2$ and [(**2**)NaBPh$_4$]$_2$ (see X-ray crystal structure determinations) are quite similar.

A sandwiching of a sodium ion within a ferrocene crown ether is only possible when one of the 1,1′-ferrocenediylbis-(methylene) bridges with its unfavorable conformational preference is exchanged by an ethanediyl group[33] –but even then not without paying a price as can be seen in the structure of (**4**)NaI (Figure 6, Table 6). The bonding of Na(1) (CN = 6–7) within the cavity of the cryptand is not symmetrical, as only one crown ether ring [N(1), O(1), O(2), N(2)] fully coordinates

(31) (a) vanRemoortere, F. P.; Boer, F. P. *Inorg. Chem.* **1974**, *13*, 2073. (b) Boer, F. P.; Neumann, M. A.; vanRemoortere, F. P.; Steiner, E. C. *Inorg. Chem.* **1974**, *13*, 2831.

(32) White, B. D.; Arnold, K. A.; Garrell, R. L.; Fronczek, F. R.; Gandour, R. D.; Gokel, G. W. *J. Org. Chem.* **1987**, *52*, 1128.

(33) Anelli, P. L.; Montanari, F.; Quici, S.; Ciani, G.; Sironi, A. *J. Org. Chem.* **1988**, *53*, 5292.

to Na(1), whereas the other displays quite an unusual conformation. One oxygen atom O(4) is situated on a crystallographic split position. O(4a) (sof = 0.6) is coordinated to Na(1), but O(4b) (sof = 0.4) is too far away [Na(1)−O(4b) = 329 pm] to contact the metal ion. The nitrogen atom N(3) within the second ring is not at all coordinated to Na(1). Another unusual feature is associated with a hydrogen atom attached to C(11), since it is located inside the cavity, right in the middle between Na(1) and Fe(1). These distortions in the structure of (**4**)NaI are due to the 1,1′-ferrocenediylbis(methylene) bridge between the two 12-membered crown ether rings. In the coordination sphere of Na(1) five atoms [Na(1), O(1), O(4a), N(1), N(4)] and four atoms [(O(2), O(3), N(2), Na(1)] lie within two different planes, which are almost perpendicular to each other. The Na(1)−O bond lengths (average 249.6 pm) are comparable to those found in [(**2**)$NaClO_4$]$_2$ and by Anelli et al. (Na−O = 246.1 pm). Anelli's ligand has two N_2-12-C-4-units linked by a C_2 and a C_3 bridge[16] and displays much longer sodium−nitrogen bonds (279.2 pm) than found in (**4**)NaI [average Na(1)−N = 250.7 pm]. It is evident from the X-ray crystal structure that the environment for Na^+ is not ideal since donor atoms are lacking; therefore Li^+ coordination is preferred.

It was first shown by Hall et al.[34] that there is a linear dependence of the charge density and the anodic shift of the redox potentials upon metal ion coordination.[13] We have recently performed a study to gain a better understanding of the effects related to the distance of the redox active center from the site of metal complexation.[35] In this investigation the protonation of ferrocene amines was used to model the electrostatic phenomena in the metal complexes of ferrocene crown ethers.

In the conformationally restricted ferrocene amines, used in our previous study, deductions from crystal structure data to structures in solution are quite reliable. This approach, however, is fraught with several problems when applied to crown ether metal complexes, since only one of several energetically accessible conformers is frozen out in a crystal. Attempts to model such complexes by molecular mechanics have been succesfully performed for the solid-state,[36,37] but the same procedure is much more difficult for processes in solution.[38] Thus knowledge of the structures of crown ether metal complexes in solution is limited.[39] This leads to the question to which extent solid-state structures actually represent the distribution of possible species in solution[40] and—related to our study—the location of the group 1A ions with respect to the redox-active center.

To contribute an answer to this question, we were interested if it was possible to correlate the metal ion (Na^+) induced shifts

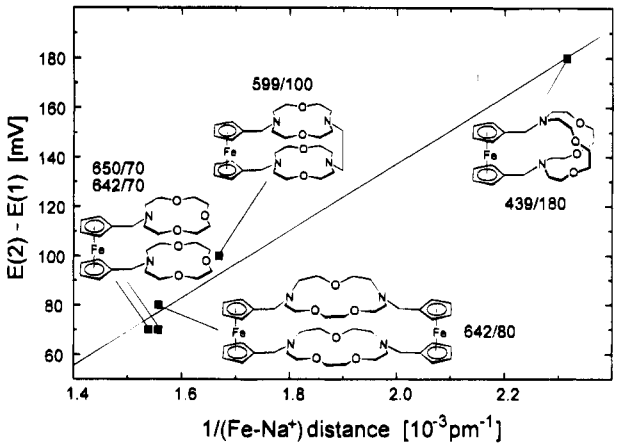

Figure 7. Plot of the reciprocal distances (Fe−Na^+) vs the differences of the redox potentials of the ferrocene crown ethers $E(1)$ and Na^+ complex of the ferrocene crown ethers $E(2)$ (Na^+ omitted).

ΔE of the redox potentials of ferrocene crown ethers with the Fe−Na^+ distances in the complex. Including the crystal structures of [(**2**)$NaClO_4$]$_2$, [(**2**)$NaBPh_4$]$_2$, and (**4**)NaI and two structures described elsewhere by Gokel et al. [(Fcdiyl(N_2-18-C-6))Na^+][13] and by us [(Fcdiyl(N_2-15-C-5)$_2$Fcdiyl)Na^+][41] (for structural diagrams see Figure 7) a total of five different Fe−Na^+ distances are available, which can be compared since the ratio of Na^+−Fe is 1 in both cases and the two iron atoms are always oxidized independently of each other. The anodic shifts ΔE of the redox potentials upon complexation of Na^+ by ferrocene crown ethers are plotted against the inverse distance (Fe−Na^+) as obtained from crystal structure analysis. $\Delta E \cong 1/(Fe-Na^+)$ is observed, thereby confirming the relation $\Delta E \cong 1/(Fe-N)$ which was found for the protonation of ferrocene amines.[35]

It is interesting that the influence of H^+ on the shifts of the redox potential falls off much more rapidly with increasing distance from the iron atom than the effect caused by Na^+. In a ferrocene amine a Fe−N distance of 437 pm corresponds to an anodic shift of 230 mV, whereas Fe−Na^+ = 439 pm in (Fcdiyl(N_2-15-C-5)$_2$Fcdiyl)Na^+ results in a shift of +180 mV. An increase in the distance Fe−N to 550 pm and Fe−Na^+ to 599 pm yields almost equal shifts of 110 mV (H^+) and 100 mV (Na^+). This could reflect the fact that upon nitrogen protonation the charge is distributed over several atoms, thus resulting in a lower effective charge density. This charge diffusion seems to be much less effective for the sodium ion.[42,43]

We are aware of the principal limitations of our attempt to correlate crystal structure data and solution measurements for metal ion complexes of crown ethers; however, the results presented here are in line with the observations made for H^+.[35]

Conclusion. The bridging of two 12-membered crown ether units by a 1,2-ethanediyl and a 1,1′-ferrocenediylbis(methylene) group results in the ferrocene cryptand **4** which displays a highly selective complexation of Li^+ versus the other group 1A ions. Li^+ can thus be detected electrochemically in the presence of all other group 1A ions, making this compound a prototype amperometric Li^+ sensor.

The anodic shifts ΔE of the redox potentials upon complexation of Na^+ by ferrocene crown ethers can be correlated with the inverse distance Fe−Na^+ as obtained from crystal structure analysis. This relationship confirms the results previously obtained for the protonation of ferrocene amines and shows that

(34) Hall, C. D.; Sharpe, N. W.; Danks, I. P.; Sang, Y. P. *J. Chem. Soc., Chem. Commun.* **1989**, 419.
(35) Plenio, H.; Yang, J.; Diodone, R.; Heinze, J. *Inorg. Chem.* **1994**, *33*, 4098.
(36) (a) Hay, B. P.; Rustad, J. R.; Hostetler, C. J. *J. Am. Chem. Soc.* **1993**, *115*, 11158. (b) Dang, L. X.; Kollman, P. A. *J. Am. Chem. Soc.* **1990**, *112*, 5716. (c) Damu, K. V.; Hancock, R. D.; Wade, P. W.; Boeyens, J. C. A.; Billing, D. G.; Dobson, S. M. *J. Chem. Soc., Dalton Trans.* **1991**, 293.
(37) Hay, B. P. *Coord. Chem. Rev.* **1993**, *126*, 177.
(38) (a) Troxler, L.; Wipf, G. *J. Am. Chem. Soc.* **1994**, *116*, 1468. (b) Wipf, G. *J. Coord. Chem.* **1992**, *27*, 7 and references therein.
(39) (a) Ratcliffe, C. I.; Ripmeester, J. A.; Buchanan, G. W.; Denike, J. K. *J. Am. Chem. Soc.* **1992**, *114*, 3294. (b) Buchanan, G. W.; Kirby, R. A.; Bourque, K. *Can. J. Chem.* **1989**, *67*, 449. (c) Live, D.; Chan, S. I. *J. Am. Chem. Soc.* **1976**, *98*, 3769.
(40) (a) Hilgenberger, R.; Saenger, W. In *Host Guest Complex Chemistry*; Vögtle, F., Weber, E., Eds.; Springer Verlag: Berlin 1985; Chapter 2. (b) Dobler, M. *Ionophores and their Structure*; Wiley Interscience: New York, 1981. (c) Kessler, H.; Zimmermann, G.; Förster, H.; Engel, J.; Sheldrick, W. S. *Angew. Chem.* **1981**, *93*, 1085; *Angew. Chem., Int. Ed. Engl.* **1981**, *20*, 1053.
(41) Plenio, H.; Diodone, R. *J. Organomet. Chem.* **1995**, *492*, 73.
(42) Koritsanszky, T.; Buschmann, J.; Luger, P.; Knöchel, A.; Patz, M. *J. Am. Chem. Soc.* **1994**, *116*, 6748.
(43) Glendening, E. D.; Feller, D.; Thompson, M. A. *J. Am. Chem. Soc.* **1994**, *116*, 10657.

crystal structures may serve as good models for species in solution. However, to better understand the association processes of metal ions and crown ethers more information on the structures in solution is required.[44]

Acknowledgment. This work was supported by the DFG through the Graduiertenkolleg "Ungepaarte Elektronen in Chemie and Biologie". We wish to thank Prof. Dr. H. Vahrenkamp for his support, Dr. W. Deck, Dr. M. Keller, and H. G. Schmidt for the collection of the X-ray data, and Dr. D. Böhler for the FAB-MS.

(44) Plenio, H.; Diodone, R. Work in progress.

Supporting Information Available: Tables of crystallograpic data, full atomic coordinates, thermal parameters, and full bond lengths and angles for all X-ray crystal strucures (28 pages). Ordering information is given on any current masthead page.

IC941449U